R-adaptivity in limit analysis

José J. Muñoz, James Hambleton and Scott W Sloan

Abstract Direct methods aim to find the maximum load factor that a domain made of a plastic material can sustain before undergoing full collapse. Its analytical solution may be posed as a constrained maximisation problem, which is computationally solved by resorting to appropriate discretisation of the relevant fields such as the stress or velocity fields. The actual discrete solution is though strongly dependent on such discretisation, which is defined by a set of nodes, elements, and the type of interpolation.

We here resort to an adaptive strategy that aims to perturb the positions of the nodes in order to improve the solution of the discrete maximisation problem. When the positions of the nodes are taken into account, the optimisation problem becomes highly non-linear. We approximate this problem as two staggered linear problems, one written in terms of the stress variable (lower bound problem) or velocity variables (upper bound problem), and another with respect to the nodal positions. In this manner, we show that for some simple problems, the computed load factor may be further improved while keeping a constant number of elements.

1 Introduction

Direct methods allow engineers and practitioners to compute the ultimate loads and determine collapse mechanisms of structures made of plastic materials. In the last twenty years, robust and efficient optimisation methods, together with appropriate

José J. Muñoz
Universitat Politècnica de Catalunya, 08036 Barcelona, Spain e-mail: j.munoz@upc.edu

James Hambleton
Dept. Civil Env. Engin., Northwestern University, USA (previously at University of Newcastle, Newcastle, Australia) e-mail: jphambleton@northwestern.edu

Scott W Sloan
University of Newcastle, Newcastle, Australia e-mail: Scott.Sloan@newcastle.edu.au

discretisations of the stress and velocity fields have, respectively, allowed for effective computing of upper and lower bounds of the load factors. The accuracy of these bounds is very much dependent on the distribution of the elements in the mesh, which should adapt to the sliplines or, more generally, the collapse mechanism.

This dependence of the the accuracy of the discrete solution on the mesh has prompted the use of adaptive meshing strategies. Among them, we highlight element subdivision based on error estimates (Muñoz et al., 2009), anisotropic strategies according to the velocity field (Lyamin et al., 2005), and fan type meshes (Lyamin et al., 2005; Muñoz et al., 2012). These strategies are applied with sequential subdivisions of the element (embedded remeshing) or by redefining an element size field and direction. In this work we propose an alternative strategy: perturbing the location of the nodes, while keeping the number of elements constant and without altering their connectivity. We in fact include the nodal positions as an additional optimisation variable in the standard upper and lower bound formulations in limit analysis. This is a similar idea to the perturbation analysis in upper bound formulations with rigid blocks introduced in Hambleton and Sloan (2013), which we here extend to more general finite elements formulations in limit analysis (Lyamin and Sloan, 2002a,b; Krabbenhøft et al., 2005; Muñoz et al., 2009).

This work is related to similar strategies where the nodal positions of the problem at hand are optimised in order to improve the accuracy of the results. This type of analysis has been so far adopted in elasticity (Thoutireddy and Ortiz, 2004), elastodynamics (Zielonka et al., 2008), analysis of stochastic materials (Cottereau and Díez, 2015) or in biomechanics (Kim et al., 2013; Ma and Klug, 2008). We here carry these ideas over to limit analysis. Instead of moving the nodes as a function of an error estimate, however, we make use of the optimisation problem in order to improve the discrete solution.

In Section 2 we revise the discrete solutions of the lower and upper bound problems in limit analysis. In Section 3 we present the extension of the previous problems for R-adaptivity. Although we have only implemented R-adaptivity for the lower bound problem, we describe the form of the upper bound solution for completeness. In Section 4 we apply the methodology to the vertical cut problem in order to test its efficiency, and Section 5 gives some final remarks.

2 Preliminaries

In this work we will restrict our attention to perfectly plastic materials whose yield criterion can be transformed as a second-order cone (SOC). In this case, upper and lower bound solutions may be written as a second-order conic programming (SOCP problem) that has the following general form,

$$\begin{aligned} \textbf{Primal: } \lambda^* = \max_{\lambda,\boldsymbol{\sigma}} \ & \lambda \\ s.t. \ & \mathbf{X}\boldsymbol{\sigma} + \lambda \mathbf{f} = \mathbf{b} \\ & \boldsymbol{\sigma} \in \mathscr{K} \end{aligned} \tag{1}$$

Here, the global vector $\boldsymbol{\sigma}$ denotes stress variables, which have been conveniently transformed in order to write the yield criterion in the form $\boldsymbol{\sigma} \in \mathscr{K}$, with $\mathscr{K}$ a second-order cone. The variable λ is the load factor, which is maximised in order to compute the ultimate load of the problem at hand.

Matrix $\mathbf{X}$ and vectors $\mathbf{f}$ and $\mathbf{b}$ depend on the discretisation of the domain, that is, on the nodal positions $\mathbf{x}$ and the triangulation $\mathscr{T}$ employed. If these are considered fixed, as it is usually the case, the problem in (1) is convex. The lower and upper formulations of limit analysis require different forms of matrix $\mathbf{X}$ and vectors $\mathbf{f}$ and $\mathbf{b}$, which may be found elsewhere (Lyamin and Sloan, 2002a,b; Krabbenhøft et al., 2005; Muñoz et al., 2009).

The problem in (1) is the standard form used for the lower bound (LB) limit analysis. The upper bound (UB) problem is generally written in the dual form of this problem, which physically corresponds to minimisation of the power dissipation. It will become convenient to derive next this dual form.

The Lagrangian function of the problem in (1) reads (Boyd and Vandenberghe, 2004):

$$\mathscr{L}(\boldsymbol{\sigma}, \lambda; \mathbf{v}, \boldsymbol{\omega}) = \lambda + \mathbf{v}^T(\mathbf{b} - \mathbf{X}\boldsymbol{\sigma} - \lambda \mathbf{f}) - \boldsymbol{\omega}^T \boldsymbol{\sigma} \tag{2}$$

The optimal value λ^* may be then obtained as

$$\lambda^* = \max_{\boldsymbol{\sigma},\lambda} \min_{\boldsymbol{\omega} \in \mathscr{K}^*, \mathbf{v}} \mathscr{L}(\boldsymbol{\sigma}, \lambda; \mathbf{v}, \boldsymbol{\omega}) = \min_{\boldsymbol{\omega} \in \mathscr{K}^*, \mathbf{v}} \max_{\boldsymbol{\sigma},\lambda} \mathscr{L}(\boldsymbol{\sigma}, \lambda; \mathbf{v}, \boldsymbol{\omega}) \tag{3}$$

where the second equality holds due to strong duality. The dual set $\mathscr{S}^*$ of a cone $\mathscr{S}$ is defined as (Boyd and Vandenberghe, 2004),

$$\mathscr{S}^* = \{\boldsymbol{\omega} | \boldsymbol{\omega}^T \boldsymbol{\sigma} \geq 0 \ \forall \boldsymbol{\sigma} \in \mathscr{S}\}$$

and for the second-order cone $\mathscr{K}$, it can be proved that $\mathscr{K}^* = \mathscr{K}$. The primal and dual problems are then obtained by keeping the maximisation or the minimisation at the left and right side of the second equality respectively. More explicitly, the primal problem in (1) may be deduced by taking derivatives of the Lagrangian with respect to the dual variables $(\mathbf{v}, \boldsymbol{\omega})$, while the dual form of the optimisation problem is obtained by taking derivatives of the Lagrangian with respect to the primal variables $(\mathbf{x}, \lambda)$, which results in,

$$\begin{aligned} \textbf{Dual: } \lambda^* = \min_{\mathbf{v}} \ & \mathbf{b}^T \mathbf{v} \\ s.t. \ & \mathbf{f}^T \mathbf{v} = 1 \\ & -\mathbf{X}^T \mathbf{v} \in \mathscr{K}^* \end{aligned} \tag{4}$$

In the previous equations, the fields $\boldsymbol{\sigma}$, $\boldsymbol{\omega}$ and $\boldsymbol{v}$ have infinite dimensions. In practice though these fields are interpolated, and depending on the interpolation used, the approximated discrete problem may yield upper, lower or non-strict estimates of the load factor. We do not detail here these interpolations which may be found elsewhere (Lyamin and Sloan, 2002a; Lyamin et al., 2005; Muñoz et al., 2009). In our examples, we will use for the lower bound a piecewise linear stress field, which is discontinuous at the element edges, and that yields strict lower bound solutions (Muñoz et al., 2009), and a piecewise linear velocity field discontinuous at the element edges, which furnishes a strict upper bound solution (Sloan and Kleeman, 1995; Muñoz et al., 2012).

3 R-adaptivity

The previous lower and upper bound problems are usually implemented by appropriately discretising the stress variable $\boldsymbol{\sigma}$ in the primal problem in (1), or by discretising the velocity field $\boldsymbol{v}$ in the dual problem in (4).

We will here present an extension of these problems that includes the nodal positions as additional variables in order to further improve the load factor estimate. Due to the non-linearity of the resulting problem and lack of convexity, the extended problem may not have a unique solution, and the bounds may not be strict. For this reason, the Lagrangian function is linearised at previous solutions.

Since the load factor must be either increased or decreased in the lower or upper bound solution, respectively, the new position variables will be either primal or dual variables in the extended problem. Although we have here implemented the lower bound extension, we present the forms of the lower and upper bound solutions for completeness.

3.1 Lower bound problem

We aim to further increase the optimal value of λ by varying the nodal positions $\mathbf{x}$. This corresponds to adding a further maximisation in (3), which now reads,

$$\lambda^{LB} = \max_{\mathbf{x}} \max_{\boldsymbol{\sigma},\lambda} \min_{\boldsymbol{\omega}\in\mathscr{K}^*,\mathbf{v}} \mathscr{L}(\boldsymbol{\sigma},\lambda,\mathbf{x};\mathbf{v},\boldsymbol{\omega})$$

From this expression, the following primal problem is proposed,

$$\begin{aligned} \lambda^{LB} = \max_{\mathbf{x},\lambda,\boldsymbol{\sigma}} \ & \lambda \\ s.t. \ & \mathbf{X}\boldsymbol{\sigma} + \lambda\mathbf{f} = \mathbf{b} \\ & \boldsymbol{\sigma} \in \mathscr{K}. \end{aligned} \tag{5}$$

It can be observed that the equality constraints above have become non-linear on the variables $\boldsymbol{\sigma}$ and $\mathbf{x}$, so that the optimisation problem is not a SOCP anymore. However, given a (non-optimal) set of primal-dual variables $(\lambda_k, \boldsymbol{\sigma}_k, \mathbf{x}_k; \mathbf{v}_k, \boldsymbol{\omega}_k)$, the Lagrangian may be linearised as follows:

$$\mathscr{L}(\boldsymbol{\sigma}, \lambda, \mathbf{x}; \mathbf{v}, \boldsymbol{\omega}) \approx \lambda + \mathbf{v}^T(\mathbf{b} - \mathbf{X}_k\boldsymbol{\sigma} - \lambda\mathbf{f}_k) - \boldsymbol{\omega}^T\boldsymbol{\sigma} - \mathbf{v}^T\left(\frac{\partial \mathbf{X}_k}{\partial \mathbf{x}}\boldsymbol{\sigma}_k + \frac{\partial \mathbf{f}_k}{\partial \mathbf{x}}\lambda_k\right)\delta\mathbf{x} \tag{6}$$

with $\delta\mathbf{x} = \mathbf{x} - \mathbf{x}_k$, and $\mathbf{X}_k$ denotes matrix $\mathbf{X}$ evaluated at the nodal positions $\mathbf{x}_k$. The approximated Lagrangian gives rise to the following primal problem:

$$\begin{aligned} \textbf{Primal(LB)-}\delta:\ \lambda^{LB} = \max_{\delta\mathbf{x},\lambda,\boldsymbol{\sigma}}\ & \lambda \\ s.t.\ & \mathbf{X}_k\boldsymbol{\sigma} + \left(\frac{\partial \mathbf{X}_k}{\partial \mathbf{x}}\boldsymbol{\sigma}_k + \frac{\partial \mathbf{f}_k}{\partial \mathbf{x}}\lambda_k\right)\delta\mathbf{x} + \lambda\mathbf{f} = \mathbf{b} \\ & \boldsymbol{\sigma} \in \mathscr{K}, ||\delta\mathbf{x}|| \leq \boldsymbol{\varepsilon} \end{aligned} \tag{7}$$

This problem has only linear and second-order constraints, and is thus a SOCP. We have added the constraint $||\delta\mathbf{x}|| \leq \boldsymbol{\varepsilon}$ in order to limit the amount of nodal perturbation $\delta\mathbf{x}$, and therefore avoid elements that are too distorted or posses negative Jacobians. Figure 1 illustrates this perturbation of the nodal positions. The matrices $\frac{\partial \mathbf{X}_k}{\partial \mathbf{x}}\boldsymbol{\sigma}_k$ and $\frac{\partial \mathbf{f}_k}{\partial \mathbf{x}}\lambda_k$ may be approximated by using numerical differentiation as follows:

$$\begin{aligned} \frac{\partial \mathbf{X}_k}{\partial x_i}\boldsymbol{\sigma}_k &\approx \frac{(\mathbf{X}_{k+\delta x_i} - \mathbf{X}_k)\boldsymbol{\sigma}_k}{\delta x_i} \\ \frac{\partial \mathbf{f}_k}{\partial x_i}\lambda_k &\approx \frac{(\mathbf{f}_{k+\delta x_i} - \mathbf{f}_k)\lambda_k}{\delta x_i} \end{aligned}$$

where matrix $\mathbf{X}_{k+\delta x_i}$ and vector $\mathbf{f}_{k+\delta x_i}$ denote $\mathbf{X}$ and $\mathbf{f}$ evaluated with the nodal coordinate x_i^k perturbed by a small quantity δx_i.

We point out that the constraints in (7) are in fact equivalent to imposing the equilibrium constraints on a moving mesh, such that the stresses and the final position of the mesh are unknown. Due to the non-linearity of these constraints, these equilibrium equations are linearised at the previous stress values $\boldsymbol{\sigma}_k$ and previous nodal positions, which gives rise to the approximated equilibrium constraints in (7). As such, this linearisation is an approximation, and thus the obtained solution may be suboptimal with respect to the analytical non-linear problem. We aim though to approach such optimal solutions as we solve successive problems from updated values of $\boldsymbol{\sigma}_k$ and $\mathbf{X}_k$.

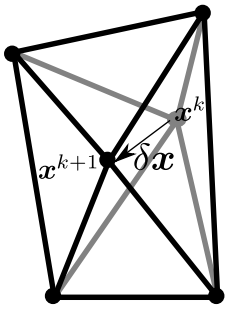

Fig. 1 Scheme of the perturbation on nodal positions. Initial nodal coordinate: $\mathbf{x}^k$. Perturbed nodal coordinate:$\mathbf{x}^{k+1} = \mathbf{x}^k + \delta\mathbf{x}$.

3.2 Upper bound problem

In contrast to the lower bound problem, we aim now to minimise the optimal value of λ (which is now an upper bound of the analytical optimal λ^*) with respect to the nodal positions $\mathbf{x}$, that is,

$$\lambda^{UB} = \max_{\boldsymbol{\sigma},\lambda} \min_{\mathbf{x}} \min_{\boldsymbol{\omega}\in\mathscr{K}^*,\mathbf{v}} \mathscr{L}(\boldsymbol{\sigma},\lambda;\mathbf{v},\boldsymbol{\omega},\mathbf{x})$$

The nodal positions thus now play the role of the dual variables $\boldsymbol{\nu}$ and $\boldsymbol{\omega}$. Thus, given a set of primal-dual solution $(\lambda_k,\boldsymbol{\sigma}_k;\mathbf{v}_k,\boldsymbol{\omega}_k,\mathbf{x}_k)$, we approximate the Lagrangian as,

$$\mathscr{L}(\boldsymbol{\sigma},\lambda;\mathbf{v},\boldsymbol{\omega},\mathbf{x}) \approx \lambda + \mathbf{v}^T(\mathbf{b}-\mathbf{X}_k\boldsymbol{\sigma}-\lambda\mathbf{f}_k) - \boldsymbol{\omega}^T\boldsymbol{\sigma} - \mathbf{v}_k^T\left(\frac{\partial\mathbf{X}_k}{\partial\mathbf{x}}\boldsymbol{\sigma}+\frac{\partial\mathbf{f}_k}{\partial\mathbf{x}}\lambda\right)\delta\mathbf{x} \tag{8}$$

From this expression, the following dual problem may be derived,

$$\begin{aligned}
\textbf{Dual(UB)-}\delta:\ \lambda^{UB} = \min_{\mathbf{v},\delta\mathbf{x}}\ & \mathbf{b}^T\mathbf{v} \\
s.t.\ & \mathbf{f}^T\mathbf{v} + \left(\mathbf{v}_k^T\frac{\partial\mathbf{f}_k}{\partial\mathbf{x}}\right)\delta\mathbf{x} = 1 \\
& -\mathbf{X}_k^T\mathbf{v} - \left(\frac{\partial\mathbf{X}_k^T}{\partial\mathbf{x}}\mathbf{v}_k\right)\delta\mathbf{x} \in \mathscr{K}^* \\
& ||\delta\mathbf{x}|| \leq \boldsymbol{\varepsilon}
\end{aligned} \tag{9}$$

where again, we have added the last constraint in order to avoid elements with large aspect ratios or a negative Jacobian. This is an extension of the dual problem in (4) for varying nodal positions $\mathbf{x}$. It can be verified that the primal form of (9) reads,

$$\begin{aligned}
\textbf{Primal(UB)-}\delta:\ \lambda^{UB} = \max_{\lambda,\boldsymbol{\sigma}}\ & \lambda - \boldsymbol{\omega}_1^T\boldsymbol{\varepsilon} \\
s.t.\ & \mathbf{X}_k\boldsymbol{\sigma} + \lambda\mathbf{f} = \mathbf{b} \\
& -\left(\mathbf{v}_k^T\frac{\partial\mathbf{X}_k}{\partial\mathbf{x}} + \lambda\mathbf{v}_k^T\frac{\partial\mathbf{f}_k}{\partial\mathbf{x}}\right)\boldsymbol{\sigma} = \boldsymbol{\omega}_2 \\
& \boldsymbol{\sigma} \in \mathscr{K} \\
& \{\boldsymbol{\omega}_1, \boldsymbol{\omega}_2\} \in \mathscr{K}_x
\end{aligned} \tag{10}$$

where the second set of constraints follows from deriving $\mathscr{L}$ with respect to the dual variable $\delta\mathbf{x}$, and $\mathscr{K}_x$ is a cone equivalent to the constraint $||\delta\mathbf{x}|| \leq \boldsymbol{\varepsilon}$. Variables $\boldsymbol{\omega}_1$ and $\boldsymbol{\omega}_2$ are new primal variables. The relative displacements are obtained from the dual variables (Lagrange multipliers) of the second set of constraints in (10).

3.3 Update of nodal positions

The analytical solution of the limit analysis yields a unique value of λ^*, but not necessarily a unique mechanism. For this reason, and due to the finite element discretisation, the optimal nodal positions $\mathbf{x}$ may differ in discrete upper and lower formulations. In our implementation, which focuses on the lower bound solution, we update the nodal positions according to

$$\mathbf{x}_{k+1} = \mathbf{x}_k + \delta\mathbf{x}^{LB} \tag{11}$$

with $\delta\mathbf{x}^{LB}$ the optimal value of the extended lower bound problem. We note though that we could alternatively modify the nodal positions according to the average of the two values of $\delta\mathbf{x}$ obtained in each case, that is according to the following vector:

$$\delta\mathbf{x} = \frac{1}{2}\left(\delta\mathbf{x}^{UB} + \delta\mathbf{x}^{LB}\right)$$

or even from a weighted average according to the gain in each bound,

$$\delta\mathbf{x} = \left(\Delta\lambda^{UB}\delta\mathbf{x}^{UB} + \Delta\lambda^{LB}\delta\mathbf{x}^{LB}\right)/\Delta\lambda$$

where $\Delta\lambda^{UB} = \lambda^{UB} - \lambda^{est}$ and $\Delta\lambda^{LB} = \lambda^{LB} - \lambda^{est}$ correspond to the error of the load factor for each discrete solution with respect to an estimate λ^{est} obtained from the evolution of each bound. In our numerical examples we have not used these averaged updates, and restricted our attention to the simplest case in (11).

As it will be shown, the effectiveness of R-adaptivity depends on the number of elements and distribution. For this reason, we have also tested the combination of R-adaptivity with *h* refinement, where the elements are subdivided according to an error estimator, as described in Muñoz et al. (2009).

4 Results

We test here R-adaptivity in order to compute the safety factor of a vertical cut subjected to an increasing gravitational field $\boldsymbol{f}$. Figure 2 shows the geometry, boundary conditions and initial mesh made of 140 elements. We have also tested an initial coarser mesh made of 28 elements, as shown in Figure 3a. In this figure, we also show with thicker (black) lines the perturbed mesh after applying R-adaptivity.

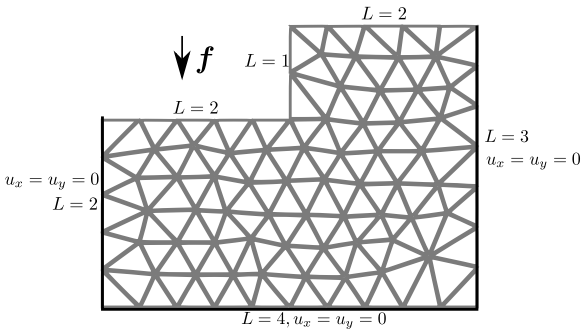

Fig. 2 Vertical cut problem. Dimensions, boundary conditions and initial mesh made of 140 elements.

The evolution of the upper and lower bounds for the initial meshes with 28 and 140 elements are shown in Figure 4a and 4b, respectively. All values plotted in this figure, including those computed from an R-adapted mesh, have been obtained using the original reduced upper and lower bound problem, without approximations arising from R-adaptivity, and are thus strict bounds. When comparing the lower bound results with respect to the evolution when only using *h*-refinement, the lower bound solution is improved with R-adaptivity: one R-adaptivity iteration is approximately equivalent to one iteration in *h*-refinement. The latter though is obtained for a higher number of elements, and thus has a higher cost. The upper bound solution though is not necessarily improved. Indeed, it appears that for a low number of elements, the improvement in the lower bound solution worsens the upper bound load factor, as one might expect given the lack of correlation between the optimal meshes for the lower and upper bound problems (see Section 3.3).

We note that the maximum nodal displacement in the extended optimisation problem, which is dictated by variable ε, is different for each node. This value is computed from the element sizes around each node. It follows that ε decreases as *h*-refinement is applied, which consequently reduces the impact of R-refinement.

We have also tested the evolution of the bounds when only using R-adaptivity. Figure 5 shows the initial and final meshes for 12 iterations of R-adaptivity. The corresponding evolution of the load factors when using a constant number of elements equal to 28 and 140 are shown in Figure 6. As before, the load factors shown are those obtained using the reduced optimisation problem (no R extension) for the

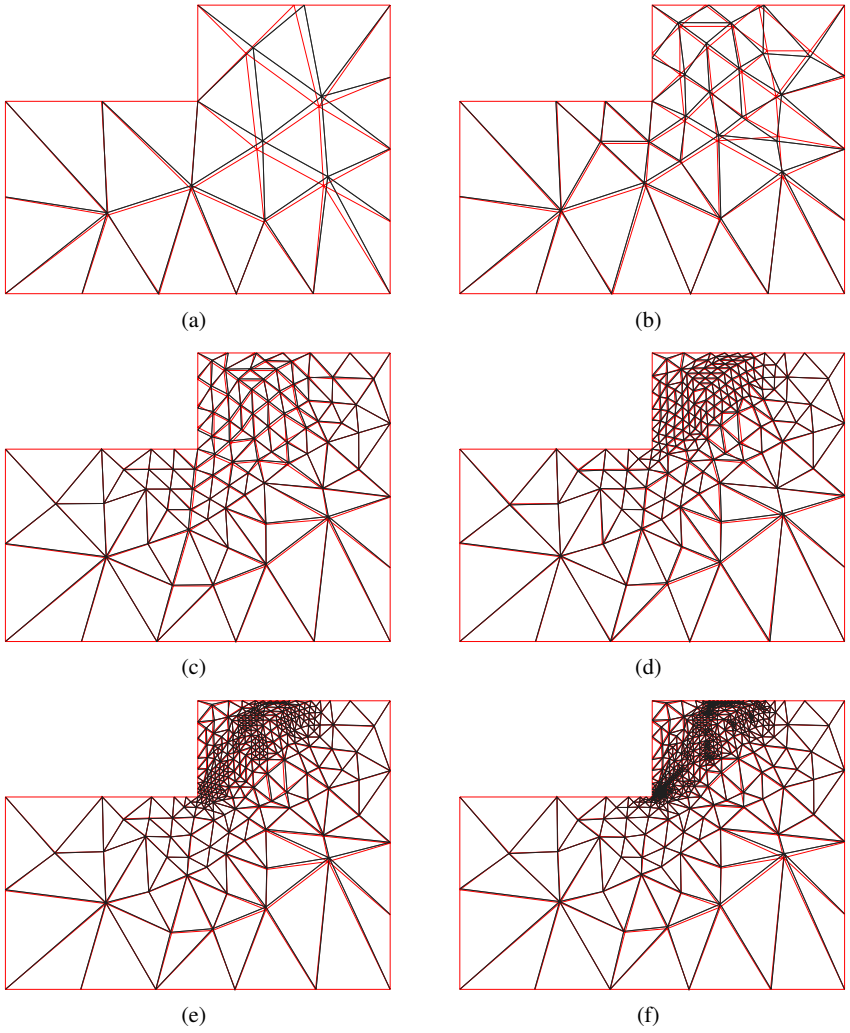

Fig. 3 Comparison of the unperturbed mesh (thinner and lighter lines) and the R-adapted mesh (thicker and darker lines) after successive h-refinements, when using an initial mesh of 28 elements. The evolution of the load factor is given in Figure 4.

new meshes, and are thus strict bounds. It can be observed the initial improvement of the lower bounds is greater for lower number of elements, but that the final gain is higher when starting with a larger number of elements, as it should be expected. Indeed, the optimal R-adapted solution in a finer mesh should be more accurate than the optimal R-adapted solution in a coarse mesh. The limitation on the values of ε (which is proportional to the mesh size) limits though the improvement in each iter-

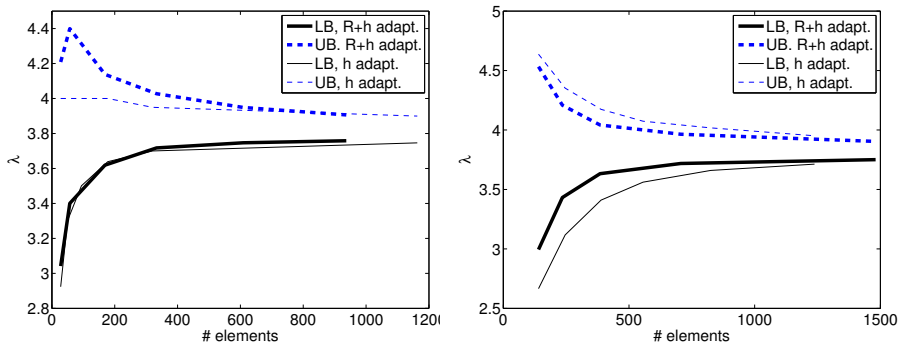

Fig. 4 Evolution of bounds for the vertical cut problem. (a): Mesh with initially 28 elements. (b):Mesh with initially 140 elements.

ation in fine meshes, and thus more iterations are required for achieving a R-adapted optimal solution.

Furthermore, after eight or nine iterations, the gain stagnates with small oscillations around an optimal solution. The fact that the extended optimisation problem in R-adaptivity is non-linear with a linearised Lagrangian, one which is only approximate, may be the cause behind these small oscillations. It can be also observed that the upper bound solution does not necessarily improve. As a final remark, we note that some of the elements achieve a high aspect ratio (Fig. 5), and could be removed from the mesh, to obtain further improvements in the computed bounds, as suggested in previous work (Hambleton and Sloan, 2013).

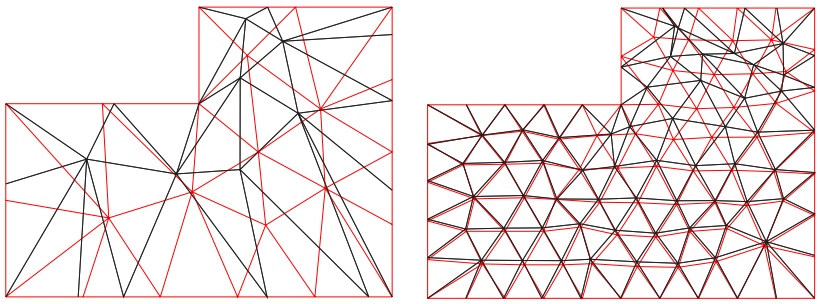

Fig. 5 Initial (thinner and lighter lines) and final (thicker and darcker lines) meshes when using R-adaptivity only. (a) Mesh with 28 elements. (b) Mesh with 140 elements. Elements with high aspect ratio can be observed on the top right side of the vertical cut.

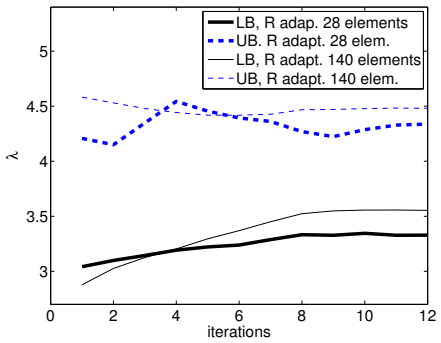

Fig. 6 Evolution of bounds when using only R-adaptivity.

5 Conclusions

In this work we have presented a remeshing strategy that extends the limit analysis optimisation problem to include the nodal positions of a given mesh in order to further improve lower and upper bound solutions of the load factor. We have derived the necessary modifications to the optimisation problems to take into account the nodal positions as additional variables, and tested the lower bound formulation.

The strategy may be combined with other error based remeshing techniques such as embedded remeshing (Muñoz et al., 2009). In these techniques, the number of elements increases, and adds new discontinuities in the discretised problem. The strategy described here aims to improve the solution and mesh distribution before further refining the mesh.

Further tests are required in order to apply R-adaptivity on the upper bound solution and wisely combine the two mesh perturbations, and also appropriately combine R-adaptivity with h-refinement. Importantly, nodal position perturbation allows us to shift the sliplines that the initial coarse meshes impose when using only embedded remeshing.

We note that the modifications of the optimisation problem are not restricted to the linear interpolations of stresses or velocities employed here. Other discretisations may be equally perturbed, and linearised on the resulting optimal variables. In addition, due to the localisation of the plastic zone, it may be advisable to allow the nodes to move only along a reduced portion of the domain, thus reducing the cost of the complete optimisation problem.

The extension of the optimisation problem with the perturbation of the nodal coordinates has an additional computational cost. This extra cost may be reduced by just adding in the optimisation process the position of those nodes that contribute to the failure mechanism, that is, that are closer to the slipline, but keeping the positions of more distant nodes unaltered. Since many geotechnical problems are driven by localised sliplines, this concentration would have a strong beneficial impact in many applications. In addition, element deletion strategies may be envisaged in order to

remove elements with high aspect ratio, as they were encountered in the final meshes when using R-adaptivity only. These strategies are currently under investigation.

References

S. Boyd and L. Vandenberghe. *Convex Optimization*. Cambridge Univ. Press, 2004.

R. Cottereau and P. Díez. Fast r-adaptivity for multiple queries of heterogeneous stochastic material fields. *Comput. Mech.*, 66:601–612, 2015.

J. Hambleton and S. Sloan. A perturbation method for optimization of rigid block mechanisms in the kinematic method of limit analysis. *Comp. Geotech.*, 48:260–271, 2013.

J. Kim, T. Panatinarak, and S. M. Shontz. A multiobjective mesh optimization framework for mesh quality improvement and mesh untangling. *Int. J. Num. Meth. Engng.*, 94(7):20–42, 2013.

K. Krabbenhøft, A. V. Lyamin, M. Hjiaj, and S. W. Sloan. A new discontinuous upper bound limit analysis formulation. *Int. J. Num. Meth. Engng.*, 63:1069–1088, 2005.

A. V. Lyamin and S. W. Sloan. Lower bound limit analysis using non-linear programming. *Int. J. Num. Meth. Engng.*, 55:576–611, 2002a.

A. V. Lyamin and S. W. Sloan. Upper bound limit analysis using linear finite elements and non-linear programming. *Int. J. Num. Anal. Meth. Geomech.*, 26: 181–216, 2002b.

A. V. Lyamin, S. W. Sloan, K. Krabbenhøft, and M. Hjiaj. Lower bound limit analysis with adaptive remeshing. *Int. J. Num. Meth. Engng.*, 63:1961–1974, 2005.

L. Ma and W. S. Klug. Viscous regularization and r-adaptive remeshing for finite element analysis of lipid membrane mechanics. *J. Comp. Phys.*, 227(11):5816–5835, 2008.

J. J. Muñoz, J. Bonet, A. Huerta, and J. Peraire. Upper and lower bounds in limit analysis: adaptive meshing strategies and discontinuous loading. *Int. J. Num. Meth. Engng.*, 77:471–501, 2009.

J. J. Muñoz, J. Bonet, A. Huerta, and J. Peraire. A note on upper bound formulations in limit analysis. *Int. J. Num. Meth. Engng.*, 91(8):896–908, 2012.

S. W. Sloan and P. W. Kleeman. Upper bound limit analysis using discontinuous velocitiy fields. *Comp. Meth. Appl. Mech. Engng.*, 127(5):293–314, 1995.

P. Thoutireddy and M. Ortiz. A variational r-adaption and shape-optimization method for finite-deformation elasticity. *Int. J. Num. Meth. Engng.*, 61:1–21, 2004.

M. G. Zielonka, M. Ortiz, and J. E. Marsden. Variational r -adaption in elastodynamics. *Int. J. Num. Meth. Engng.*, 74:1162–1197, 2008.

References

S. Boyd and L. Vandenberghe. *Convex Optimization*. Cambridge Univ. Press, 2004.

R. Cottereau and P. Díez. Fast r-adaptivity for multiple queries of heterogeneous stochastic material fields. *Comput. Mech.*, 66:601–612, 2015.

J. Hambleton and S. Sloan. A perturbation method for optimization of rigid block mechanisms in the kinematic method of limit analysis. *Comp. Geotech.*, 48:260–271, 2013.

J. Kim, T. Panatinarak, and S. M. Shontz. A multiobjective mesh optimization framework for mesh quality improvement and mesh untangling. *Int. J. Num. Meth. Engng.*, 94(7):20–42, 2013.

K. Krabbenhøft, A. V. Lyamin, M. Hjiaj, and S. W. Sloan. A new discontinuous upper bound limit analysis formulation. *Int. J. Num. Meth. Engng.*, 63:1069–1088, 2005.

A. V. Lyamin and S. W. Sloan. Lower bound limit analysis using non-linear programming. *Int. J. Num. Meth. Engng.*, 55:576–611, 2002a.

A. V. Lyamin and S. W. Sloan. Upper bound limit analysis using linear finite elements and non-linear programming. *Int. J. Num. Anal. Meth. Geomech.*, 26: 181–216, 2002b.

A. V. Lyamin, S. W. Sloan, K. Krabbenhøft, and M. Hjiaj. Lower bound limit analysis with adaptive remeshing. *Int. J. Num. Meth. Engng.*, 63:1961–1974, 2005.

L. Ma and W. S. Klug. Viscous regularization and r-adaptive remeshing for finite element analysis of lipid membrane mechanics. *J. Comp. Phys.*, 227(11):5816–5835, 2008.

J. J. Muñoz, J. Bonet, A. Huerta, and J. Peraire. Upper and lower bounds in limit analysis: adaptive meshing strategies and discontinuous loading. *Int. J. Num. Meth. Engng.*, 77:471–501, 2009.

J. J. Muñoz, J. Bonet, A. Huerta, and J. Peraire. A note on upper bound formulations in limit analysis. *Int. J. Num. Meth. Engng.*, 91(8):896–908, 2012.

S. W. Sloan and P. W. Kleeman. Upper bound limit analysis using discontinuous velocitiy fields. *Comp. Meth. Appl. Mech. Engng.*, 127(5):293–314, 1995.

P. Thoutireddy and M. Ortiz. A variational r-adaption and shape-optimization method for finite-deformation elasticity. *Int. J. Num. Meth. Engng.*, 61:1–21, 2004.

M. G. Zielonka, M. Ortiz, and J. E. Marsden. Variational r -adaption in elastodynamics. *Int. J. Num. Meth. Engng.*, 74:1162–1197, 2008.